

Based on observations made at GEMINI-S, NOAO Proposal
ID 2010B-0183.

The First Fluorine Abundance Determinations in Extragalactic AGB Carbon Stars

C. Abia¹

Dpto. Física Teórica y del Cosmos, Universidad de Granada, 18071 Granada, Spain

`cabia@ugr.es`

K. Cunha²

National Optical Astronomy Observatory, P.O. Box 26732, Tucson, AZ 85726, USA

S. Cristallo^{1,*}

Dpto. Física Teórica y del Cosmos, Universidad de Granada, 18071 Granada, Spain

***Present address: INAF-Osservatorio di Collurania, 64100 Teramo, Italy**

P. de Laverny³

*University of Nice-Sophia Antipolis, CNRS (UMR 6202), Cassiopée, Observatoire de la
Côte d'Azur, B.P. 4229, 06304 Nice Cedex 4, France*

I. Domínguez¹

Dpto. Física Teórica y del Cosmos, Universidad de Granada, 18071 Granada, Spain

A. Recio-Blanco³

*University of Nice -Sophia Antipolis, CNRS (UMR 6202), Cassiopée, Observatoire de la
Côte d'Azur, B.P. 4229, 06304 Nice Cedex 4, France*

V.V. Smith²

National Optical Astronomy Observatory, P.O. Box 26732, Tucson, AZ 85726, USA

and

O. Straniero⁵

INAF-Osservatorio di Collurania, 64100 Teramo, Italy

ABSTRACT

Fluorine (^{19}F) abundances (**or upper limits**) are derived in **six** extragalactic AGB carbon stars from the HF(1-0) R9 line at $2.3358\ \mu\text{m}$ in high resolution spectra. The stars belong to the Local Group galaxies LMC, SMC and Carina dwarf spheroidal, spanning more than a factor 50 in metallicity. This is the first study to probe the behaviour of F with metallicity in intrinsic extragalactic C-rich AGB stars. Fluorine could be measured only in four of the target stars, showing a wide range in F-enhancements. Our F abundance measurements together with those recently derived in Galactic AGB carbon stars show a correlation with the observed carbon and *s*-element enhancements. The observed correlations however, display a different dependence on the stellar metallicity with respect to theoretical predictions in low mass, low metallicity AGB models. We briefly discuss the possible reasons for this discrepancy. If our findings are confirmed in a larger number of metal-poor AGBs, the issue of F production in AGB stars will need to be revisited.

Subject headings: stars: abundances — stars: carbon — stars: AGB and post-AGB — galaxies: individual (LMC, SMC, Carina) — nuclear reactions, nucleosynthesis, abundances

1. Introduction

Comparisons between abundances of some key elements determined in stars in different evolutionary stages with nucleosynthetic stellar models is a fundamental tool for our understanding of stellar interiors. One element that can add new insight into this is fluorine, since this element is very sensitive to nuclear reactions involving proton and/or alpha captures. Actually, the origin of this light element is still uncertain although much observational progress has been made in recent years in cool K, M and Asymptotic Giant Branch (AGB) stars (e.g. Jorissen et al. 1992, hereafter JSL; Cunha et al. 2003-08; Smith et al. 2005; Uttenthaler et al. 2008), and in post-AGB stars and planetary nebulae (Werner et al. 2005; Otsuka et al. 2008). From these observational studies two conclusions are derived: i) AGB stars constitute the only evidence of stellar F production and, ii) the inferred evolution of the F abundance in the Galaxy, when compared with chemical evolution models (Renda et al. 2004), requires the contribution of the additional sources proposed so far: gravitational supernovae (Woosley et al. 1990) and Wolf-Rayet stars (Palacios et al. 2005).

Evidence of F production in AGB stars was found by JSL two decades ago: F enhancements up to a factor 30 solar and a correlation of F with the C/O ratio was first reported in Galactic (O-rich & C-rich) AGB stars of solar metallicity. Since the C/O ratio is expected to increase in the envelope during the AGB phase as a consequence of the third dredge-up (TDU) episodes, this was interpreted as evidence of F production. The F enhancements found by JSL, however, could not be accounted by detailed models for AGB stars at that epoch (Mowlavi et al. 1998), or by more recent ones (Lugaro et al. 2004) that included the impact of the variation of some nuclear reactions with uncertain rates affecting F. Nonetheless, a recent re-analysis of the JSL’s stars by Abia et al. (2009-10; hereafter Paper I and II) using improved line lists and model atmospheres found that the F abundances reported in JSL have been overestimated because of a possible lack of proper accounting for C-bearing molecule blends. This reanalysis reported F abundances by ~ 0.7 dex lower on average. The new F abundances and the observed correlation between F and *s*-element enhancements in solar metallicity C-stars, are now fully accounted by the current nucleosynthetic modelling of low mass AGB stars (Cristallo et al. 2009-11).

At low metallicities the situation is less clear. Theoretically, the F production in AGB stars is expected to increase when decreasing metallicity. AGB stars synthesise F via $^{14}\text{N}(n, p)^{14}\text{C}(\alpha, \gamma)^{18}\text{O}(p, \alpha)^{15}\text{N}(\alpha, \gamma)^{19}\text{F}$ and $^{14}\text{N}(\alpha, \gamma)^{18}\text{F}(\beta^+)^{18}\text{O}(p, \alpha)^{15}\text{N}(\alpha, \gamma)^{19}\text{F}$, where the neutrons are provided by $^{13}\text{C}(\alpha, n)^{16}\text{O}$ and the protons mainly by $^{14}\text{N}(n, p)^{14}\text{C}$. Thus, the production of F basically depends on the availability of ^{13}C in the He-rich intershell, but also on the amount of ^{13}C available in the ashes of the H-burning shell. The former is weakly dependent on the stellar metallicity but the latter scales with the CNO abundances in the envelope, which, in turn, depends on the (primary) ^{12}C dredged up during TDU episodes. As a consequence, the resulting fluorine can be roughly considered a primary element. Because of this primary nature, larger $[\text{F}/\text{Fe}]^1$ ratios are obtained in metal-poor, low-mass AGB models as compared with the solar metallicity case. Nonetheless, the available determinations of F abundances in low metallicity stars depict a more complex scenario than that expected from this simple theoretical **scheme**. For instance, Cunha et al. (2003) derived $[\text{F}/\text{O}] \lesssim 0.0$ in RGB stars of ω Cen *enriched* in *s*-process elements, which is difficult to reconcile with metal-poor AGB stars being significant F contributors. Recently, Lucatello et al. (2011) found lower $[\text{F}/\text{Fe}]$ ratios than theoretically expected in a sample of Galactic carbon enhanced metal-poor stars enriched in *s*-elements (CEMP-*s*). The implications of these findings are not easy: first, the surface composition in the ω Cen giants is hampered by the uncertain star formation history and chemical evolution of this cluster and, on the

¹We adopt the usual notation with $[x/y] = \log [N(x)/N(y)]_{\star} - \log [N(x)/N(y)]_{\odot}$ and $\log \epsilon(x) = 12 + \log [N(x)/N(H)]$.

other hand, the abundances measured in CEMP-s stars (mostly binaries) **might be affected by the** dilution of the accreted material onto the envelope of the secondary star. The amount of material accreted is uncertain and, thus are **in general** the interpretation of the abundances. On the contrary, F abundances derived in intrinsic metal-poor AGB stars, i.e. stars which own their chemical peculiarities to internal nucleosynthesis, are free of these problems². Unfortunately, the few metal poor Galactic AGB stars, as those observed in globular clusters, have masses too low to undergo TDU events and thus, to pollute the envelope with the nucleosynthesis ashes of the He-rich intershell. For this reason, the AGB C-stars in the satellite galaxies of the Milky Way offer a unique opportunity to study the ¹⁹F production at low metallicity. These galaxies are well known to content metal-poor stellar populations.

Here we present for the first time F abundance measurements in metal-poor AGB carbon stars in stellar systems other than the Galaxy: the SMC, LMC and Carina dSph galaxies. These C-stars are significantly more metal poor than the Galactic counterparts so far analysed providing valuable information on how F is produced in AGB stars as a function of metallicity.

2. Observations and Analysis

The stars were chosen from previous optical high-resolution spectroscopic studies of extragalactic AGB C-stars (de Laverny et al. 2006; Abia et al. 2008). In addition to the stars analysed there (BMB B30 belonging to the SMC, and ALW-C6 and ALW-C7 to Carina dSph), we added two stars in the LMC (TRM88 and MSX663) and a new target in the SMC (GM780). Details about the characteristics of BMB B30, ALW-C6 and ALW-C7 can be found in the above works (the other stars are described below). The stars were observed in classical mode with the 8.1 m Gemini-South telescope and the Phoenix spectrograph (Hinkle et al. 1998) at a resolving power $R \sim 50,000$; and centred at 23350 \AA , to include the HF(1-0) R9 line. In Paper I it was shown that this line is the most reliable for F abundance determinations in cool stars. A detailed description of the Phoenix observations and the corresponding data reduction can be found in Smith et al. (2002). Table 1 shows the exposure times for each object, and the signal-to-noise ratios reached in the final spectrum.

Two target stars are peculiar: MSX663 is a long-period variable classified as a S star by Cioni et al. (2001) (C-rich but with $C/O < 1$). Zijlstra et al. (2006) indicated that this

²In Section 3 we show that the $[F/Fe]$ ratio achieved in the envelope in the C-rich AGB phase is almost independent on the initial F content in the star.

object may be a symbiotic star. Surprisingly, our spectrum of this object shows no spectral lines in the $2.3 \mu\text{m}$ region; even the vibration-rotation CO lines, usually strong, are absent. This might be compatible with this object being a supergiant rather than an AGB star. In any case, we could not identify the R9 line and thus, it was discarded for analysis. GM780 is also a rare object. Lagadec et al. (2007) noted that the C_2H_2 bands, commonly observed in C-stars, were absent. Also, the $J - K$ colour of this object (2.6), is quite red, and dust should be present around it. These authors concluded that GM780 has a C/O ratio considerably lower than that in any other star in their sample. Our high-resolution spectrum confirms this finding; all the features of CN and C_2 molecules in the $2.3 \mu\text{m}$ region appear very weak. Also, the high excitation CO lines look broader and affected by line doubling. Actually, a much larger macroturbulence value than typical one was required to fit the line profiles in this star. We do not know the reason of this, but the effect of dust or/and stellar pulsation might be at play (see e.g. Nowotny et al. 2011). In fact, our synthetic fit to its spectrum was not satisfactory.

The classical method of spectral synthesis was used in the analysis. Theoretical LTE spectra were computed in spherical geometry and convolved with Gaussian functions to mimic the corresponding instrumental profile adding a macroturbulence velocity typically of $5 - 7 \text{ km/s}$ (a 10 km/s value was used for GM780). For more details on the method of analysis, and the adopted molecular and atomic line lists used see Paper I. We adopted the atmospheric parameters derived in de Laverny et al. (2006) and Abia et al. (2008) for the stars BMB B30, ALW-C6 and ALW-C7, and followed the same procedure to derive the stellar parameters in the remaining stars (see these works for details). Accordingly, we estimate a $T_{eff} \sim 2000 \text{ K}$ for GM780 (note the red $J - K$ colour of this star), and 3400 K for TRM88. Since our grid of C-rich atmosphere models (Gustafsson et al. 2008) does not include a T_{eff} as low as 2000 K , we used a model with such a T_{eff} from the C-rich models grid by Pavlenko & Yakovina (2010). A gravity of $\log g = 0.0$ and a $\xi = 2.2 \text{ km/s}$ were adopted for all the stars (see e.g. Lambert et al. 1986). The analysis of BMB B30, ALW-C6 and ALW-C7 resulted in different C/O ratios than those previously derived from optical spectra. These differences were, nevertheless, within the uncertainties³. Unfortunately, the observed spectral range does not contain useful metallic lines to estimate the metallicity ($[\text{Fe}/\text{H}]$) in the stars TRM88 and GM780. Thus, we initially adopted the metallicity of the main stellar population in the LMC and SMC ($[\text{Fe}/\text{H}] \sim -0.4$ and -0.7 , respectively). Then,

³The derived C/O ratios have an additional uncertainty since the O abundance cannot be determined independently of the C abundance. This is because theoretical spectra are almost insensitive to a large variation of the O abundance provided that the difference $\log \epsilon(\text{C}-\text{O})$ is kept constant. **The estimated error in the C and O abundances is ± 0.3 dex. See de Laverny et al. (2006) and Paper I for details.**

comparisons of synthetic to observed spectra provided new estimates of the metallicity by assuming that the O abundance derived from CO lines is an indication of the metallicity. This procedure was repeated until a good fit to the full spectrum was obtained. Despite the O abundance might not be a good indicator of the metallicity, note that variations in the metallicity of the model atmosphere scale linearly to the F abundance derived. This means that the $[F/Fe]$ ratio is almost independent of the metallicity adopted in the model atmosphere.

Figure 1 shows examples of synthetic fits in the R9 line region for the stars TRM88 and ALW-C7. The blend to the left wing of the HF line has a significant contribution of $^{12}C^{17}O$. This feature allowed to derive the $^{16}O/^{17}O$ ratio (see Table 1) in the most metallic stars of the sample. In the most metal-poor objects (stars in Carina) however, this blend is insensitive to variations of the $^{16}O/^{17}O$ ratio. For some of the targets, Na abundances were also derived from the Na I line at $\lambda 23379$ Å. This line is, however, blended with molecular features, thus its detection depends on the current Na abundance in the star (see Table 1). For each element (and the $^{16}O/^{17}O$ ratio), the uncertainty was calculated by determining individually the sensitivities of the derived abundance to the adopted T_{eff} , gravity, C and O abundances, microturbulence, and metallicity. We then sum in quadrature the resulting uncertainties associated to each parameter. The synthetic fit to the HF and the Na I lines is particularly sensitive to the T_{eff} adopted, the other parameters affecting at a lower degree (**in particular gravity and metallicity, see Paper I**). The resulting formal uncertainty is ± 0.30 dex for F, ± 0.26 dex for Na, and a factor ~ 2 for the $^{16}O/^{17}O$ ratio.

3. Results and Discussion

Table 1 summarises the main results. We find a wide range in $[F/Fe]$ ratios in metal-poor extragalactic AGB C-stars. Fluorine is enhanced in all except one star, confirming that this element is produced during the AGB phase. Figure 2 provides further evidence of this. The similarity in the run of F with C strongly support that the synthesis of F is tied to the production of C during the Thermal Pulsing (TP) AGB phase. Also Figure 2 qualitatively shows that F enhancement increases for decreasing stellar metallicity (although the star B30 seems to deviate from this trend). In Paper II we showed that at solar metallicity, the F and C correlation can be reproduced by current TP-AGB models (Cristallo et al. 2009, continuous lines in Figure 2). Models and observations, however, now seem to disagree in metal-poor AGB stars (dashed lines); theoretical models tend to overproduce C for a given F enhancement. Indeed, the two stars in Carina should be along the model computed with $Z \sim 10^{-4}$ (right dashed line), while the star B30 along the model line with $Z \sim 10^{-3}$. This

discrepancy, which has been already noted at solar Z (e.g. Abia et al. 2002), becomes more evident at lower metallicity as Figure 2 shows, since in current AGB models the efficiency of the TDU increases at low metallicity and thus, the amount of C dredged-up into the envelope. Note that this problem could be also an observational bias: intrinsic AGB C-stars with high C/O ratios should exist, as high values of C/O have been observed both in post-AGB stars and in extrinsic C-rich objects originated by mass transfer from an AGB star. However, in cool C-stars an excess of carbon is immediately translated into a copious production of C-rich dust and into a high opacity of the circumstellar environment, to the point of hiding the photosphere at visual wavelengths. Most of the C might be trapped into grains. These dusty C-stars should show large infrared excess. Curiously enough, the two stars in our sample (Table 1) with high C/O ratios do not show this as deduced from their available infrared photometry, while the star GM780, with large infrared excess (see Section 2) has the typical $C/O \gtrsim 1$ ratio observed in C-stars.

Figure 3 provides another piece of information on the synthesis of F in AGB stars. It shows the observed relation between F and the average⁴ s -element enhancements in C-stars of different metallicities compared with theoretical predictions. Again the observed trend **points-out** to a correlation between $[F/Fe]$ and $[\langle s \rangle/Fe]$. Despite the scarce number of metal-poor objects studied, the observations suggest a different dependence than that theoretically expected (Cristallo et al. 2011) as a function of the metallicity: in metal-poor C-stars larger $[F/Fe]$ ratios are expected for the observed s -element enhancement. While the F and Na enhancements⁵ found in ALW-C7 can be simultaneously accounted (within error bars) by our reference $1.5 M_{\odot}$, $Z \sim 10^{-4}$ TP-AGB model, the predicted $[\langle s \rangle/Fe]$ ratio is lower than the observed value. It is a challenge that the same models which nicely reproduce the trend found at solar metallicity (lower dashed line in Figure 3), fail in reproducing the metal-poor data. This discrepancy can also be noticed in Figure 4, where the $[F/\langle s \rangle]$ ratios found in Galactic CEMP-s (Lucatello et al. 2011) and intrinsic AGB C-stars are plotted. Note that by plotting the $[F/\langle s \rangle]$ ratio we avoid any dilution problem that may affect the abundances derived in CEMP-s stars. From this figure, it is clear again that the F content derived in metal-poor stars is lower than the predicted values.

Now the question is how to account for these apparent low F enhancements? In the recent years, some degree of extramixing processes have been invoked to explain the $^{16}O/^{17}O/^{18}O$ ratios found in grains of AGB origin, and the low $^{12}C/^{13}C$ ratios in C-stars (Busso et al. 2010). Extramixing has been proposed by Denissenkov et al. (2006) **as a pos-**

⁴Obtained as the mean value of the $[Sr, Zr, Y, Ba, La, Nd, Sm/Fe]$ ratios.

⁵Na can be also produced during the TP-AGB phase, see Cristallo et al. (2009).

sible solution⁶ of the observed anti-correlation of F and Na abundances found in low-mass giants of M4 (Smith et al. 2005). Extramixing might reduce F in the AGB envelope if such processes expose material at temperatures high enough to activate the $^{19}\text{F}(p, \alpha)$ reaction. However, the $^{16}\text{O}/^{17}\text{O}$ ratios found in TRM88 and B30 are those characteristic of stars which have undergone the first dredge-up. The measurement of the $^{16}\text{O}/^{18}\text{O}$ ratio in these stars would be critical to give a definite answer on the occurrence or not of extramixing processes but, unfortunately, ^{18}O could not be determined. Even the large (> 100) $^{12}\text{C}/^{13}\text{C}$ ratio found in B30 (de Laverny et al. 2006) cannot add any hint on the presence of extramixing, due to the larger $^{12}\text{C}/^{13}\text{C}$ ratios attained on the surface according to metal-poor AGB models already after the first TDUs. On the other hand, several nuclear reaction rates affecting F are still uncertain, in particular $^{15}\text{N}(\alpha, \gamma)^{12}\text{C}$. We performed **preliminary** tests with nuclear rates modified within the current uncertainties and found that this can only mildly improve the situation but actually it seems not enough to solve the problem. Another possibility is that these metal-poor C-stars formed with an initial F abundance much lower than the one scaled to their metallicity (see Section 1). Note that the chemical evolution of these satellite galaxies is essentially unknown (even the run of F with $[\text{Fe}/\text{H}]$ in our Galaxy is uncertain). Nonetheless, according to our theoretical metal-poor AGB models the F production is so large that the $[\text{F}/\text{Fe}]$ ratio reached in the envelope in the C-rich phase ($\text{C}/\text{O} > 1$) is independent of the initial F content in the star. For instance, in a $1.5 M_{\odot}$, $Z \sim 10^{-3}$ AGB model assuming an initial $[\text{F}/\text{Fe}] = -1.0$, the predicted $[\text{F}/\langle s \rangle]$ ratio after a few TPs **differs less than 0.1 dex with respect to that obtained with a solar scaled initial ratio. The difference is even smaller for lower metallicity models.**

In summary, from the comparison between the derived F abundances and the current models we conclude that the F synthesis in metal-poor AGB stars is probably not **as large as expected or some physical mechanism, not currently considered in the models, efficiently destroys it**. Obviously, additional F abundance measurements in metal-poor AGB stars would be extremely important to enlighten this problem. The origin of this element still remains unknown.

Part of this work was supported by the Spanish grants AYA2008-04211-C02-02 and FPA2008-03908 from the MEC. P. de Laverny and A. Recio-Blanco acknowledge the financial support of Programme National de Physique Stellaire (PNPS) of CNRS/INSU, France. S.C and O.S. have been partially supported by the italian MIUR grant FIRB-Futuro in ricerca 2008. We are thankful to B. Plez for providing us molecular line lists in the observed infrared domain and to K. Eriksson and Y. Pavlenko for the metal-poor C-rich atmosphere models.

⁶There are other explanations more widely accepted, see e.g. Marino et al. (2008).

Facilities: GEMINI-S (Phoenix).

REFERENCES

- Abia, C., et al. 2002, ApJ, 578, 817
- Abia, C., de Laverny, P., & Whalin, R. 2008, A&A, 481, 161
- Abia, C., et al. 2009, ApJ, 694, 971 (Paper I)
- Abia, C., et al. 2010, ApJ, 715, L94 (Paper II)
- Asplund, M., Grevesse, N., Sauval, J.A., & Scott, P. 2009, ARAA, 47, 481
- Busso, M., et al. 2010, ApJ, 717, L47
- Cioni, M.R., et al. 2001, A&A, 377, 945
- Cristallo, S., et al. 2009, ApJ, 696, 797
- Cristallo, S., et al. 2011, ApJ, submitted
- Cunha, K., Smith, V.V., Lambert, D.L., & Hinkle, K.H. 2003, AJ, 126, 1305
- Cunha, K., & Smith, V.V. 2005, ApJ, 626, 425
- Cunha, K., Smith, V.V., & Gibson, B. 2008, ApJ, 679, L17
- de Laverny, P., et al. 2006, A&A, 446, 1107
- Denissenkov, P.A., Pinsonneault, M., & Terndrup, D.M. 2006, ApJ, 651, 438
- Goriely, S., & Mowlavi, N. 2000, A&A, 362, 599
- Gustafsson, B. et al. 2008, A&A, 486, 951
- Hinkle, K.H., et al. 1998, Proc. SPIE, 3354, 810
- Jorissen, A., Smith, V.V., & Lambert, D.L. 1992, A&A, 261, 164 (JSL)
- Lagadec, E., et al. 2007, MNRAS, 376, 1270
- Lambert, D.L., Gustafsson, B., Eriksson, K, Hinkle, K.H. 1986, ApJS, 62, 373
- Lucatello, S., et al. 2011, ApJ, 729, 40

- Lugaro, M. et al. 2004, ApJ, 615, 934
- Marino, A. F. et al. 2008, A&A, 490, 625
- Mowlavi, N., Jorissen, A., & Arnould, M. 1998, A&A, 334, 153
- Nowotny, W., Aringer, B., Höfner, S., & Lederer, M.T. 2011, A&A, 529,
- Otsuka, M., Izumiura, H., Tajitsu, A., & Hyung, S. 2008, ApJ, 682, L108
- Palacios, A., Arnould, M., & Meynet, G. 2005, A&A, 443, 243
- Pavlenko, Y. A., & Yakovina, L. 2010, Kinematics & Physics of Celestial Bodies, 25, 302
- Renda, A., et al. 2004, MNRAS, 354, 575
- Smith, V.V., et al. 2002, AJ, 124, 3241
- Smith, V.V., et al. 2005, ApJ, 633, 392
- Uttenthaler, S. et al. 2008, ApJ, 682, 509
- Werner, K., Rauch, T., & Kruk, J.W. 2005, A&A, 433, 641
- Woosley, S.E., et al. 1990, ApJ, 356, 272
- Ziljstra, A., et al. 2006, MNRAS, 370, 1961

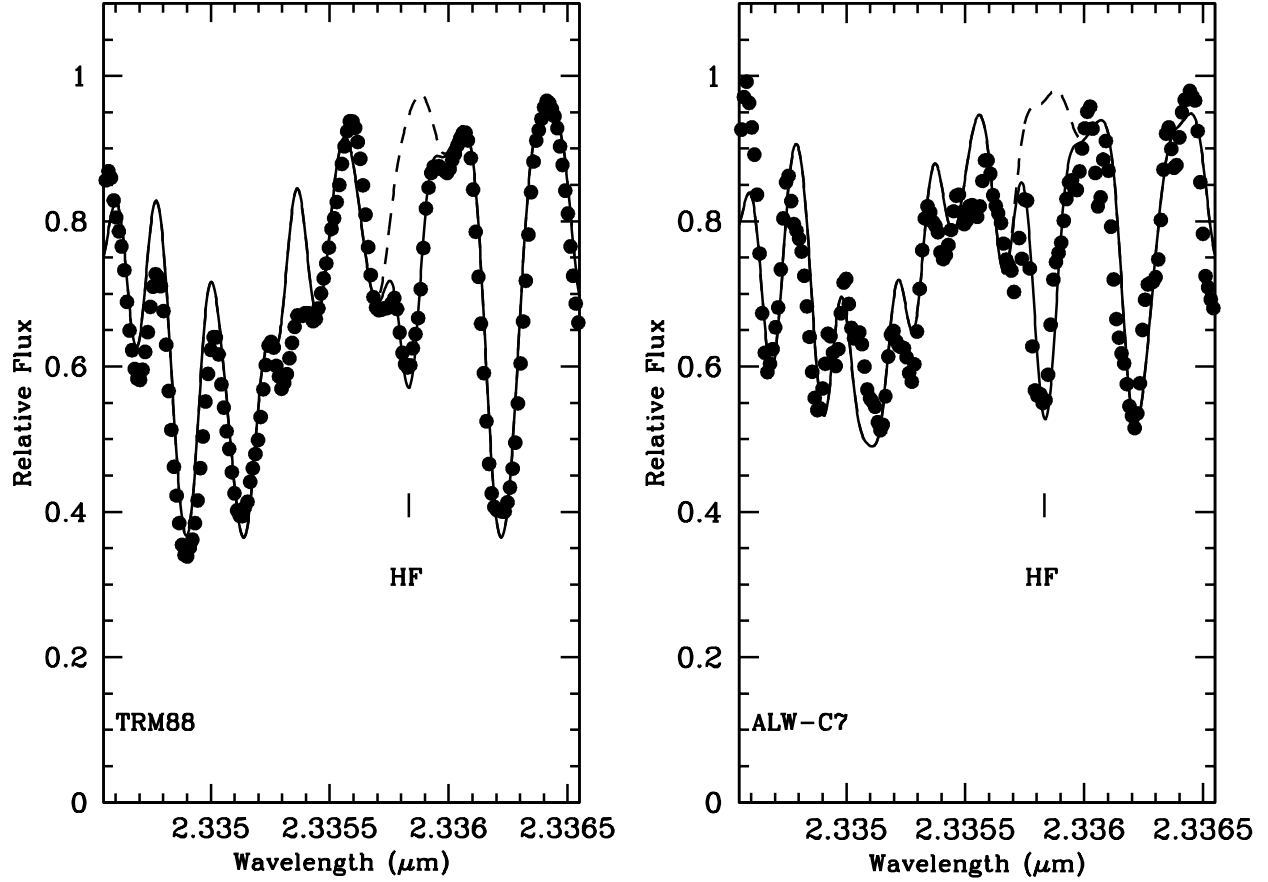


Fig. 1.— Observed spectra in the region of the HF R9 line of the stars TRM88 and ALW-C7 (black dots) compared to their best fit model spectra (continuous lines) computed with the corresponding F abundances (see Table 1). Synthetic spectra computed with no F (dashed lines) are also shown. Note the more noisy spectrum of ALW-C7.

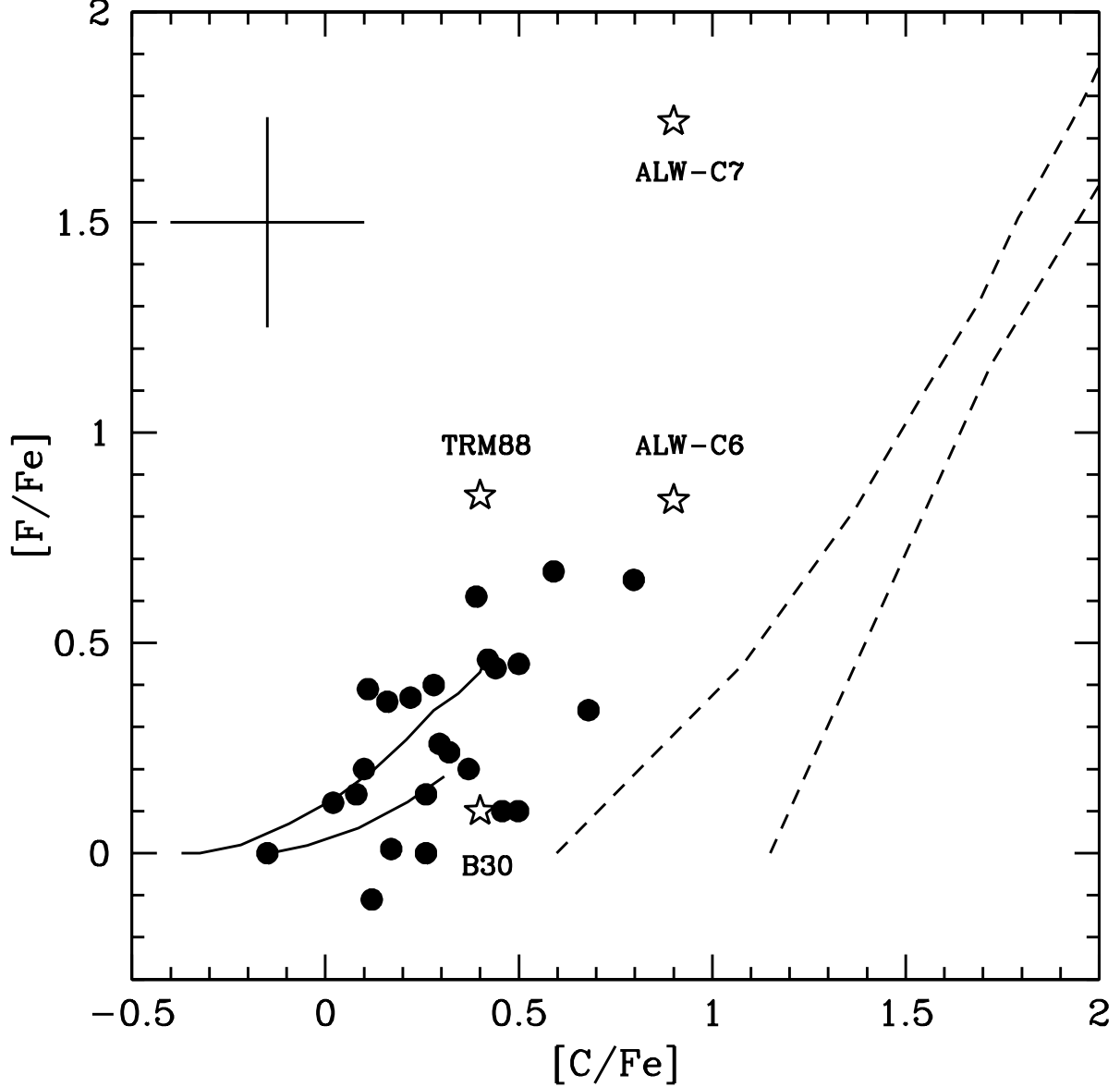


Fig. 2.— Observed $[F/Fe]$ vs. $[C/Fe]$ ratios in Galactic (dots, from Paper II) and extragalactic (open stars, this study) N-type AGB carbon stars. Lines are theoretical predictions for a $2 M_{\odot}$ and $1.5 M_{\odot}$ TP-AGB model with $Z = Z_{\odot}$ (left and right continuous lines, respectively) and for a $1.5 M_{\odot}$ model with $Z = 10^{-3}$ and 10^{-4} (left and right dashed lines, respectively). Note that for the $[F/Fe]$ ratios derived in the metal-poor extragalactic carbon stars the predicted C enhancement is much larger than observed (see text).

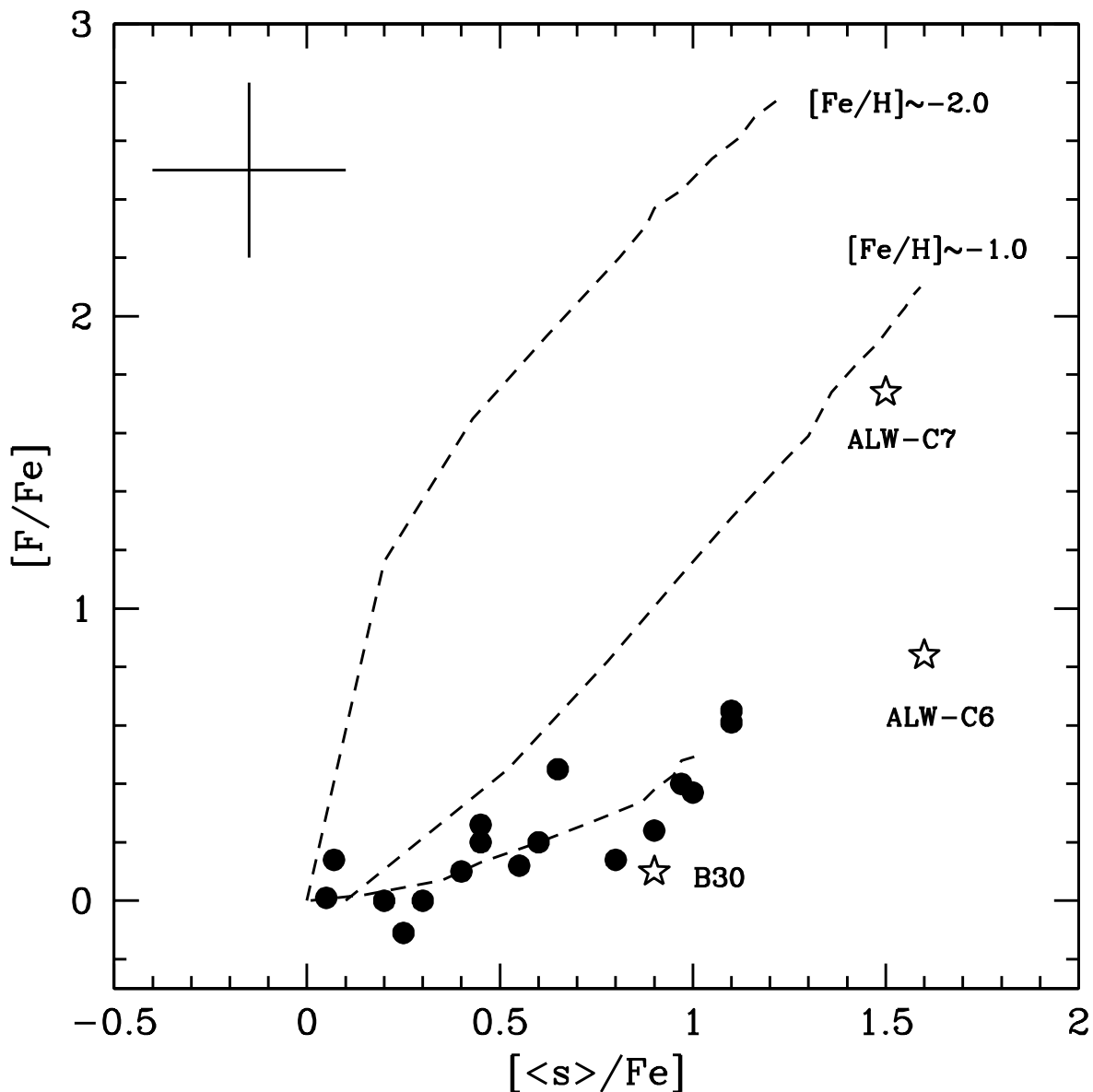


Fig. 3.— Fluorine vs. average s -element enhancements in Galactic and extragalactic AGB carbon stars. Symbols as in Figure 2. Dashed lines are theoretical predictions for a $1.5 M_{\odot}$ TP-AGB model for different metallicities ($[\text{Fe}/\text{H}] \sim 0.0, -1.0, -2.0$ from bottom to up) according to Cristallo et al. (2011) (see text). The $\langle s \rangle / \text{Fe}$ ratios in the extragalactic stars are from de Laverny et al. (2006) and Abia et al. (2008), while those in Galactic stars from Abia et al. (2002).

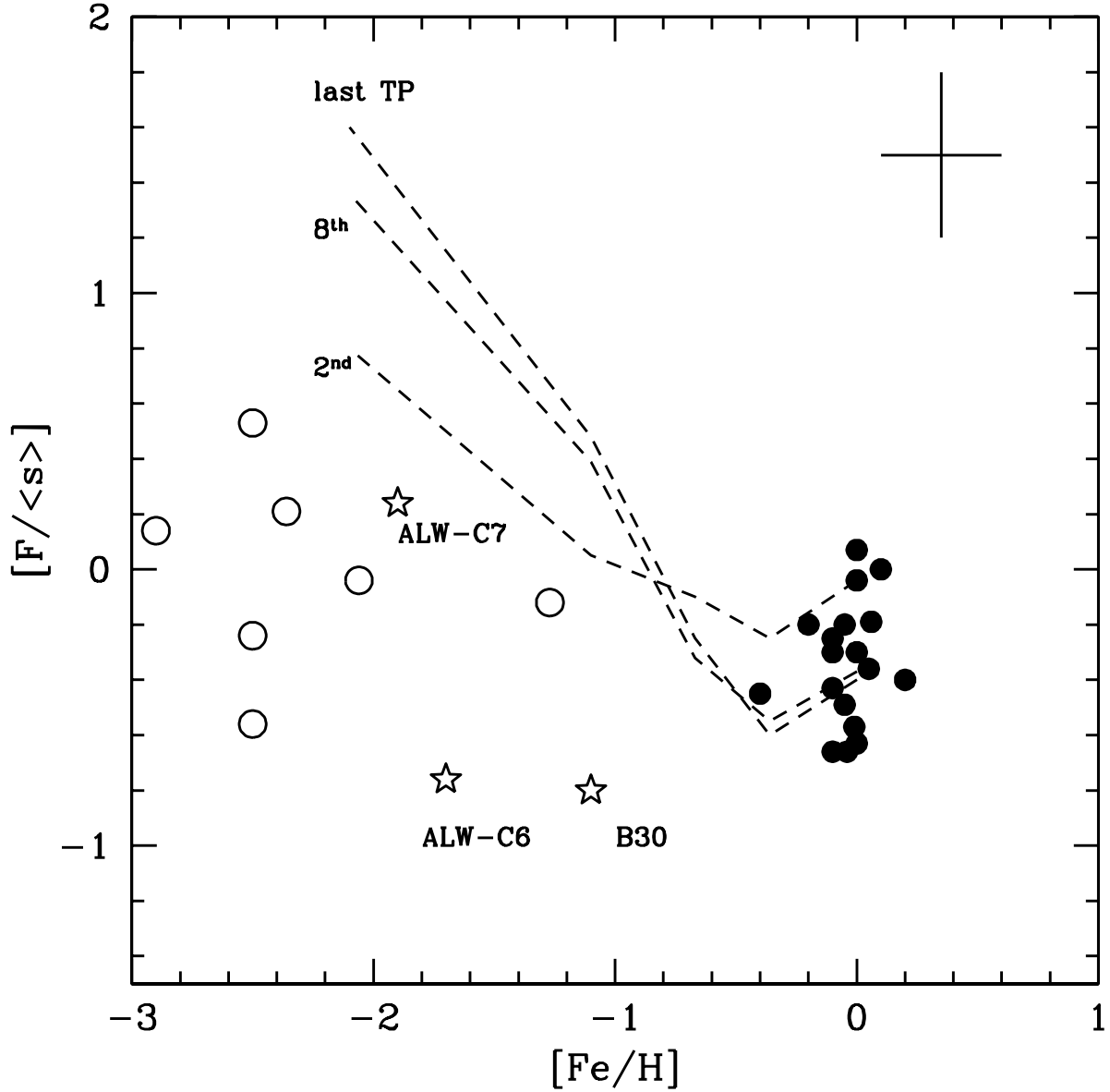


Fig. 4.— Observed $[F/\langle s \rangle]$ vs. $[Fe/H]$ ratios in intrinsic AGB carbon stars (symbols as in Figure 2) and extrinsic CEMP-s stars (open circles, from Lucatello et al. 2011 and references therein) compared with theoretical predictions (dashed lines) at several thermal pulses (2^{nd} , 8^{th} and last TP) for a $1.5 M_{\odot}$ TP-AGB model with different metallicities.

Table 1. Data and Abundances for Program Stars^a

Star	K	Exp. time (s)	S/N	T_{eff}	[Fe/H]	C/N ^b /O	$\log \epsilon(\text{C-O})$	$^{16}\text{O}/^{17}\text{O}$	$\log \epsilon(\text{F})$	$\log \epsilon(\text{Na})$	[F/Fe]	[Na/Fe]	[<s>/Fe] ^d
LMC TRM88	10.30	5400	55	3400	-0.6	8.20/7.25/8.05	7.63	425	4.85	5.40	+0.85	-0.24	...
LMC MSX663 ^c	10.20	5400	57 / ... /
SMC BMB-B30	10.70	6300	65	3000	-1.1	7.70/6.83/7.60	7.05	440	3.60	5.20	+0.14	0.06	+0.90
SMC GM780 ^d	10.25	3600	67	2000	-1.3	7.45/6.50/7.40	6.81	...	<3.26	<4.80	<0.0	<-0.14	...
Carina ALW-C6	12.30	9000	35	3400	-1.7	7.60/6.10/6.70	7.54	...	3.70	<4.50	+0.84	<0.0	+1.60
Carina ALW-C7	12.70	7200	30	3200	-1.9	7.40/5.83/6.40	7.35	...	4.40	5.30	+1.74	+0.96	+1.50

^aThe adopted solar abundances are from Asplund et al. (2009).

^bN abundances are scaled to the stellar metallicity.

^cThe average s-element enhancements are taken from de Laverny et al. (2006) for BMB B30, and Abia et al. (2008) for the stars in Carina.

^dThe star LMC MSX663 shows no spectral lines in the 2.3350 μm region and was discarded for abundance analysis (see text).

^eThe atmospheric parameters adopted for this star and the derived abundances have to be considered as very uncertain (see text).